



**Environmental
Science**
Nano

Mechanism of zinc oxide nanoparticle entry into wheat seedling leaves

Journal:	<i>Environmental Science: Nano</i>
Manuscript ID	EN-ART-06-2020-000658.R1
Article Type:	Paper

SCHOLARONE™
Manuscripts

Environmental Significance Statement

Nanoparticles are increasingly used in agriculture by the advance in nanotechnology to improve plant health, plant growth, and food security. Many kinds of metallic nanoparticles could benefit the plant health as foliage nano-fertilizers without any abiotic stress at proper concentrations. The understanding of the mechanisms on their transport, dissolution, and distribution in plant leaves is important, however, the related investigation is rather limited. This work reports the process of ZnO NPs uptake, dissolution, and distribution in wheat seedling leaves. The results will help to understand the mechanism of ZnO NPs uptake and distribution in plant leaves and provide important information on the sustainable use of ZnO NPs and potentially other soluble NPs in agriculture.

Mechanism of zinc oxide nanoparticle entry into wheat seedling leaves†

Jiahui Zhu,^{ab} Jinfeng Li,^a Yu Shen,^{a,c} Shiqi Liu,^a Nengde Zeng,^a Xinhua Zhan,^{*a} Jason C. White,^c Jorge Gardea-Torresdey,^d and Baoshan Xing^{*b}

* Corresponding author: Prof. Xinhua Zhan

Phone: +86-25-84395210

E-mail: xhzhan@njau.edu.cn

* Corresponding author: Prof. Baoshan Xing

Tel.: +1 (413) 545-5212

E-mail: bx@umass.edu

1
2
3
4 **ABSTRACT:** Nanoparticles (NPs) are increasingly used as agrochemical components
5
6 through foliar spraying such as foliage-fertilizers or pesticides. However, an understanding
7
8 of the mechanisms of nanoparticle absorption and translocation from the leaf surface is
9
10 limited. In this study, ZnO NPs (30 nm) labeled with fluorescein isothiocyanate (FITC) were
11
12 foliarly applied to wheat leaf tissues to investigate the process of attachment and absorption.
13
14 Using laser confocal microscopy, we observed that FITC-ZnO NPs cross the leaf epidermis
15
16 through the stomata and accumulate first in the apoplast, followed by subsequent transport
17
18 to mesophyll cells. The Zn concentrations in wheat leaf apoplast and cytoplasm decreased
19
20 33.2% and 8.3% with stomatal aperture diameter reduction, respectively; the apoplastic Zn
21
22 concentration is influenced more by stomatal aperture than the cytoplasmic Zn level.
23
24 Scanning electron microscopy with energy-dispersive X-ray analysis was used to map Zn in
25
26 the wheat leaves and data suggest a different Zn distribution for ZnO NPs and ZnSO₄. Zn
27
28 ions in ZnO NP-treated samples are heterogeneously distributed in comparison with ZnSO₄
29
30 treated samples. The results indicate that the main route to cross wheat leaf epidermis for
31
32 ZnO NPs is *via* stomata, then these nanoparticles accumulate and release Zn ions in the
33
34 apoplast, and the released Zn ions and ZnO NPs are absorbed by mesophyll cells. Our
35
36 findings demonstrate how ZnO NPs cross the wheat leaf epidermis, distribute within
37
38 mesophyll tissues, and enter into plant cells; and this information is useful for the
39
40 development of sustainable nano-enabled platforms for nanoscale micronutrient delivery.
41
42
43
44
45
46
47
48
49
50
51

52
53
54
55 **KEYWORDS:** *ZnO NPs, foliar application, absorption pathway, translocation, Zn*
56
57 *distribution, wheat leaves*
58
59
60

Introduction

Nanotechnology offers broad developments in agricultural applications.¹ There are several possible pathways for nanoparticle use in agriculture including as nano-fertilizers,² nano-pesticides,³ and nano-enabled environmental restoration.⁴ A large number of studies have demonstrated that at an appropriate dose, nanoparticles may have positive effects on seed germination,⁵ plant growth, yield,⁶ and resistance.⁷

Zn is an essential mineral nutrient for plant growth and is involved in a broad range of physiological processes, including reproductive organ development, secondary metabolism, and tolerance to biotic/abiotic stress.⁸ The background concentration and high variability of Zn and the growing conditions have important effects on the fate of Zn in plants.⁹ Several studies with wheat have demonstrated that Zn can improve seed germination, seedling growth and productivity, chlorophyll and grain Zn concentration, leaf area, and the photosynthetic rate.¹⁰⁻¹³ Foliar and soil applications are the two primary methods for zinc fertilizer.¹⁴ Compared to soil application, foliar application of zinc fertilizer is a potentially more effective way to deliver the nutrient to plants.¹⁵ At present, zinc oxide and zinc sulfate are the primary forms of zinc fertilizer used with plants.^{14,16} Zinc sulfate has the characterizations of high solubility and high rate of absorption, which could induce phytotoxicity.¹⁷ In fact, this is a problem encountered for most fertilizers and pesticides. Zinc oxide nanoparticles (ZnO NPs) are one of the common forms of zinc addition in agriculture, and a number of previously published studies indicated that ZnO NPs have greater positive impact and accumulation in plants (wheat, coffee, peanut and maize) than ZnSO₄.^{8,18-20} Several studies have demonstrated positive effects on plant growth at relatively low

1
2
3
4 concentrations.^{18,21,22} For example, foliar spray of ZnO NPs (13 nm) to *Arachis hypogaea*
5
6 (peanut) at 10-30 mg L⁻¹ increased Zn concentration (4.5-5.6 folds), as well as other growth
7
8 parameters such as plant height (1.2-1.4 folds) and fresh weight (1.7-2.4 folds).²³ Significant
9
10 increases in shoot height (31.51%), root length (66.29%), and plant biomass (27.1%) of
11
12 cluster bean were observed after receiving a foliar application of 10 mg L⁻¹ ZnO NPs (3.8
13
14 nm).²⁴ Under field conditions, Subbaiah et al.⁸ observed that the yield of maize grain and the
15
16 zinc concentration were increased by foliar application of 400 mg L⁻¹ ZnO NPs (25 nm).
17
18 Based on these studies, it seems likely that ZnO NPs at the appropriate dose may serve as a
19
20 kind of nano-fertilizer which can benefit plant growth with minimal abiotic stress.
21
22 Importantly, the mechanisms of ZnO NP attachment, dissolution, absorption, and
23
24 translocation in plants remains poorly understood.
25
26
27
28
29
30
31

32
33 A number of studies have focused on the effects of nanoparticles on plants, including
34
35 reports on the foliar absorption of nanoparticles such as mesoporous silica nanoparticles,²⁵
36
37 fullerenes,²⁶ titanium dioxide nanoparticles (TiO₂ NPs),²⁷ and copper oxide nanoparticles
38
39 (CuO NPs).²⁸ Some plants like soybean could absorb fertilizers by trichomes, but most crops
40
41 have two main potential routes for foliar-applied NPs entry: the stomata and the cuticle. It
42
43 was reported that stomata aperture generally ranges from 3.5 to 100 μm.²⁹ Several reports
44
45 have focused on the stomatal pathway as the probable route for the absorption of
46
47 microparticles³⁰ and nanoparticles^{22,28} by leaves. These studies indicated that the
48
49 nanoparticles may be absorbed by plant leaves through stomata. Pores in the cuticle are small
50
51 (ranging from about 0.2 to 2 nm) and have a reported size-exclusion limit in the nanometer
52
53 range.³¹ This means that ions can transport through the hydrophilic cuticular pores,³² but
54
55
56
57
58
59
60

1
2
3
4 most nanoparticles are hard to be absorbed through these pores. Maybe some nanoparticles
5
6 in a very small size could expand the cuticular pores, but the evidence is limited. However,
7
8 particle dissolution on the plant surface could also be a part of the absorption process and has
9
10 been described for ZnO NPs, copper oxide nanoparticles and cerium dioxide nanoparticles
11
12 (CeO₂ NPs).^{19,32-34} As such, the absorption of insoluble NPs such as silica NPs, fullerene,
13
14 gold nanoparticles (Au NPs) and titanium dioxide nanoparticles is more straightforward, and
15
16 the accumulation of soluble NPs may occur by multiple pathways.
17
18
19
20
21

22 Because ZnO NPs are relatively hydrophilic and little evidence supports that NPs could
23
24 enlarge cuticle pores, we hypothesize that the main route for ZnO NPs entry into wheat leaves
25
26 is *via* stomata. To address these mechanistic questions about the absorption, translocation
27
28 and distribution of ZnO NPs in wheat seedling leaves, we foliarly applied ZnO NPs onto
29
30 wheat leaves under different degrees of stomatal aperture to investigate the processes of
31
32 absorption and translocation over time. Elucidation of the uptake and translocation pathways
33
34 for ZnO NPs into wheat leaves will provide valuable and necessary information for the
35
36 development of nano-enabled agricultural applications.
37
38
39
40
41
42
43
44
45
46
47

48 **Material and methods**

49 **Chemicals and plants preparation**

50 ZnO NPs were purchased from Shanghai Aladdin Bio-Chem Technology Co., Ltd (30 ± 10
51
52 nm, purity ≥ 99%). TEM and SEM images indicate that the size of ZnO NPs is around 30 nm
53
54 (Fig. S7†). Fluorescein isothiocyanate (FITC), dimethyl formamide (DMF) and 3-
55
56
57
58
59
60

1
2
3
4 aminopropyl triethoxy silane (APTES) were purchased from Shanghai Sangon Biotech Co.,
5
6 Ltd. ABA was purchased from Sigma-Aldrich Corporation (purity \geq 98%). MTs were
7
8 purchased from Shanghai Yuanye Bio-Technology Co., Ltd (purity \geq 95%). RNAiso Plus,
9
10 primescriptTM RT Master Kit and TB[®] Premix Ex TaqTM II were purchased from Takara,
11
12 China. Primers for *HAI* (GenBank: FB811310.1), *Metallothionein (class II)* (GenBank:
13
14 X68289.1) and *Actin* (GenBank: AB181991.1) were synthesized by Shanghai Sangon
15
16 Biotech Co., Ltd.
17
18
19
20
21

22 Wheat (*Triticum aestivum* L. cv. NAU 9918) was chosen as the model plant for this work;
23
24 3% H₂O₂ was used to sterilize wheat seeds for 5 min, followed by rinsing thoroughly with
25
26 deionized water. Seeds were then germinated in dark surroundings at 25 °C for 2 days. The
27
28 germinated seeds were grown in vermiculite in a growth chamber (14 h light, 25 °C)/10 h
29
30 dark (20 °C) and relative humidity of 75% with a light intensity of 400 $\mu\text{mol m}^{-2} \text{s}^{-1}$). After 5
31
32 days, all the wheat seedlings were transferred into aerated Hoagland nutrient solution (pH
33
34 5.5) in a growth chamber with the same growth conditions as the aforementioned for
35
36 additional 5 days (at the two to three-leaf stage).
37
38
39
40
41
42
43
44

45 **Fluorescent labeling of ZnO NPs**

46
47 The labeling of ZnO NPs was performed as previously reported.³⁵ Twenty mg of bare ZnO
48
49 NPs were dispersed in 15 mL anhydrous dimethylformamide (DMF). A solution of 2.5 μL
50
51 3-aminopropyl triethoxy silane (APTES) dissolved in 125 μL DMF was then added to the
52
53 ZnO NPs suspension, followed by sonication and stirring for 24 h in the water bath (25 °C,
54
55 100 W, 40 kHz). The functionalized ZnO NPs were collected by centrifugation (3000 g, 15
56
57
58
59
60

1
2
3
4 min) and were re-suspended in 2.5 mL DMF prior to mixing with a solution of 5 mg FITC
5
6 in 5 mL DMF. The suspension was sonicated and stirred for 4 h in the water bath (25 °C, 100
7
8 W, 40 kHz). After thoroughly washing the stained ZnO NPs with DMF, 30 mL of deionized
9
10 water was added to the FITC-labeled ZnO NPs. The process was repeated until no
11
12 fluorescence was detected in the supernatant; the labeled nanoparticles were then dried under
13
14 vacuum and stored as dry powders in the dark at 4 °C.
15
16
17
18
19
20
21

22 **Assays for the characterizations of ZnO and FITC-ZnO NPs**

23
24 Zeta potential, hydrodynamic and dissolution of ZnO and FITC-ZnO NPs were determined
25
26 by previously reported methods.³⁶ ZnO and FITC-ZnO NPs (100 µmol L⁻¹) were suspended
27
28 in deionized water. The suspensions of ZnO and FITC-ZnO NPs were dispersed by ultrasonic
29
30 treatment (25 °C, 100 W, 40 kHz) with stirring for 1 h to achieve a stable dispersion. After
31
32 that, the hydrodynamic diameter and zeta potential of ZnO and FITC-ZnO NPs dispersed
33
34 solutions were determined with a Zetasizer system (Malvern Instrument Ltd., Worcestershire,
35
36 UK). The pH and conductivity of NPs suspension and ZnSO₄ solution (100 µmol L⁻¹) were
37
38 measured by the pH/conductivity meter (Thermo scientific Orion star, USA).
39
40
41
42
43
44

45
46 The time-dependent dissolutions of ZnO and FITC-ZnO NPs were measured in deionized
47
48 water.³⁷ The solutions of ZnO and FITC-ZnO NPs were dispersed with ultra-sonicator (25
49
50 °C, 100 W, 40 kHz) with stirring for 1 h before use. Samples were collected at five time
51
52 points (2, 4, 8, 16 and 24 h); the samples were filtered through 0.45 µm glass filter after being
53
54 centrifuged at 8000 g for 15 min and then acidified with 1 mol L⁻¹ HNO₃. The time-dependent
55
56 dissolutions of ZnO NPs at pH 5.8 and 7.5 were measured in this study, and the preparation
57
58
59
60

1
2
3
4 of determined solution was the same as the above. The yields of ZnO NPs (solid) after
5
6 centrifugation at different pH values were shown in the table (Table S2†). Due to the high
7
8 solubility of ZnO NPs in acid solution (Fig. S6†), the yield at pH 5.8 was lower than that at
9
10 pH 7.0 or 7.5. Zn²⁺ concentrations were determined with a flame atomic absorption
11
12 spectrophotometer (FAAS) (AAS, Z-2000, Hitachi, Japan). The working curve of FASS is
13
14 shown in the Supporting Information (Fig. S8†).
15
16
17
18
19
20
21

22 **Measurement of stomatal aperture**

23
24 The measurement method for stomatal aperture was taken from the literatures with some
25
26 modifications.^{38,39} Wheat leaves were treated with 100 μmol L⁻¹ ABA (spraying) under the
27
28 light conditions for 2 h. The wheat leaves were cut into rectangular sections. The lower
29
30 epidermis from the middle of leaf was peeled with a tweezer along the edge, and then put
31
32 into the buffer (10 mmol L⁻¹ KCl, 5 mmol L⁻¹ 2-(N-morpholino) propanesulfonic acid (MES),
33
34 and pH 6.5). Afterward, the sample was transferred on microscopy slides with a coverslip on
35
36 the top of the hypodermis. Images of each treatment were taken under a light microscope
37
38 (Nikon ECLIPSE 80i, Japan) attached with a CCD (charge coupled device) camera. ImageJ
39
40 software was used to measure the stomatal aperture. 30 stomata were selected and measured
41
42 for each treatment.
43
44
45
46
47
48
49
50
51
52

53 **Imaging of ZnO NPs in wheat leaf tissues by confocal laser scanning microscope**

54
55 A method of wheat leaf tissue sectioning was used from the literature with modifications.⁴⁰
56
57 Specifically, the wheat leaves with similar chlorophyll content and size were divided into
58
59
60

1
2
3
4 two groups. The control and treated groups were sprayed with deionized water and 100 μmol
5
6 L^{-1} ABA solution (40 μL per exposed leaf) on the leaves, respectively. After 2 h, 100 μmol
7
8 L^{-1} FITC-ZnO NPs suspension (40 μL per exposed leaf) was sprayed on wheat leaves in all
9
10 groups. All the solutions/suspensions were sprayed with small hand-held spray bottles. Most
11
12 of the spray reached the wheat leaves by this application method.⁴¹ Sampling was performed
13
14 by using a cork borer at different time points (2, 4, 8, 16 and 24 h) after foliar application.
15
16 Then, all leaf tissues were mounted on microscope slides after being rinsed with deionized
17
18 water and dried. Very few ZnO NPs were found on the washed surface of wheat leaves (Fig.
19
20 S9†). An observation gel well (5 mL neutral resins for every 1 mL xylene, 1 mm thin) was
21
22 made for mounting the wheat leaf discs. The leaf tissue was placed in the center of the
23
24 observation gel. Afterward, a coverslip was placed on the top of the leaf tissue carefully to
25
26 seal it into the well, ensuring that no bubbles remain trapped underneath. All the prepared
27
28 sample slides were evaluated with a white light laser confocal microscope (TCS SP8,
29
30 Germany). A 40 \times objective was used in the observation. The excitation/emission
31
32 wavelengths for FITC and chloroplast were 488/519 nm and 488/650 nm in the laser confocal
33
34 microscopic observation, respectively. Five sample slides from each treatment were used for
35
36 observing.
37
38
39
40
41
42
43
44
45
46
47
48
49
50

51 **Scanning electron microscope and energy disperse spectroscopy image**

52
53 Zn distribution in wheat leaf tissues was investigated by an ultra-high resolution (1.0 nm)
54
55 scanning electron microscopy (Hitachi SU8010, Japan). Specifically, fresh wheat leaf tissues
56
57 were treated with 1 mmol L^{-1} ZnO NPs and ZnSO_4 by small sprayers for 24 h and 48 h,
58
59
60

1
2
3
4 respectively. All suspensions and solutions were sprayed with the same volume (40 μL per
5
6 exposed leaf) at the uniform rate by small hand-held spray bottles. The majority of the spray
7
8 reached the wheat leaves through this application method.⁴¹ Thereafter, all samples were
9
10 washed with deionized water and cut into small pieces (about 10 mm long). These tissue
11
12 segments were frozen in liquid nitrogen, shifted into a vacuum sample exchange chamber.
13
14 The samples were cut by a knife installed in the vacuum sample exchange chamber, and then
15
16 kept under vacuum for 30 min to evaporate the ice. The cryo-based techniques retained the
17
18 structural integrity of leaf cells. Scanning electron microscopy–energy dispersive X-ray
19
20 spectroscopy (SEM-EDS and elemental mapping) was then used to detect and map the
21
22 distribution of Zn in wheat leaf tissues.⁴²
23
24
25
26
27
28
29
30
31

32 **Assays for Zn concentration in wheat leaves**

33
34
35 The measurement of Zn concentration in wheat leaves was conducted as described in the
36
37 literature with modification.^{43,44} The wheat leaves with similar chlorophyll content and size
38
39 were employed. The selected wheat seedlings were divided into four groups. Group one was
40
41 treated with deionized water (40 μL per exposed leaf); group two was treated with 100 μmol
42
43 L^{-1} ABA solution (40 μL per exposed leaf); group three was treated with deionized water (40
44
45 μL per exposed leaf) for 2 h, and then treated 100 $\mu\text{mol L}^{-1}$ ZnO NPs suspension (40 μL per
46
47 exposed leaf); and group four was treated with 100 $\mu\text{mol L}^{-1}$ ABA solution (40 μL per
48
49 exposed leaf) for 2 h, and then treated with 100 $\mu\text{mol L}^{-1}$ ZnO NPs suspension (40 μL per
50
51 exposed leaf). All suspensions and solutions were sprayed with small hand-held spray bottles.
52
53
54
55
56
57
58 Most of the spray reached the wheat leaves using this application method.⁴¹ All groups were
59
60

1
2
3
4 sampled at different time points (2, 4, 8, 16 and 24 h) after spraying ZnO NPs, and then were
5
6 successively washed by deionized water to minimize the ZnO NPs adsorbed on the leaf
7
8 surface (Fig. S9†) on the clean experimental table. The sampled wheat leaf tissues (1 g) were
9
10 put in 50-mL glass beakers and were infiltrated three times with 50 mmol L⁻¹ MES-Tris
11
12 buffer solution (pH 6.5) at 0.1 mol L⁻¹ Pa for 15 min. The leaf tissues were then transferred
13
14 into 5 mL-plastic needle tubes which were then placed into 15-mL plastic centrifuge tubes
15
16 with the point side down. All tubes were centrifuged at 4000 g for 20 min at 4 °C to collect
17
18 the apoplastic fluids.⁴⁴ After repeating the extraction process for three times, the leaf tissues
19
20 in needle tubes were then frozen at -20 °C for 72 h. The cytoplasmic fluid 1 was collected
21
22 from the frozen-thawed samples by centrifugation at 4000 g (4 °C) for 20 min. The tissues
23
24 were homogenized in 1 mL MES-Tris buffer solution (pH 6.5) for 5 min. After centrifuging
25
26 (4000 g, 4 °C), supernatants were collected as cytoplasmic fluid 2. The combined two
27
28 supernatants represented the cytoplasmic fluids. Subsequently, all apoplastic and
29
30 cytoplasmic fluids were digested with a 10-mL mixture acid of HClO₄ and HNO₃ (1:4) at the
31
32 controlled temperature of 160 °C.⁴⁵ After filtration through 0.45 μm glass filters, the Zn
33
34 concentration in apoplastic and cytoplasmic fluids was determined by FAAS as the above
35
36 described.
37
38
39
40
41
42
43
44
45
46
47
48
49

50 **Quantitative real-time PCR analysis, enzyme activity determination**

51
52 Primers for target genes *HAI* (GenBank: FB811310.1), *Metallothionein (class II)* (GenBank:
53
54 X68289.1) and the reference gene *Actin* (GenBank: AB181991.1) were synthesized by
55
56 Shanghai Sangon Biotech Co., LTD. The total RNA was isolated by using Total RNA
57
58
59
60

1
2
3
4 Extractor (Takara Bio, China). The cDNA of target genes for quantitative detection was
5
6 transcribed from total RNA using the PrimeScriptTMMRT reagent Kit (Takara Bio, China).
7
8 After real-time PCR amplification (ABI 7500/7500 Real-Time PCR System), the data were
9
10 collected and the expression level of target genes was calculated by the $2^{-\Delta\Delta C_t}$ method.⁴⁶
11
12
13

14 The activity of P-type ATPase was measured according to the previous study.⁴⁷ Wheat leaf
15
16 tissues were homogenized in a buffered medium (pH 8.0, 0.25 mol L⁻¹ sucrose, 10% glycerol,
17
18 0.1 mol L⁻¹ Mops, 1,3-bis(tris [hydroxymethyl] methylamino) propane (BTP), 2 mmol L⁻¹
19
20 EDTA, 2 mmol L⁻¹ dithiothreitol, 2 mmol L⁻¹ phenylmethylsulfonyl fluoride, 0.4%
21
22 polyvinylpyrrolidone-40T, 0.3% bovine serum albumin, and 0.1 mol L⁻¹ KCl). A miracloth
23
24 membrane was used to filter the homogenate. The filtrate was then collected and used for
25
26 centrifugation to obtain the microsomal fraction. After centrifugation, the microsomal
27
28 fraction was transferred into a separate centrifuge tube and dissolved in a buffer (15%
29
30 glycerol, 20 mmol L⁻¹ Tris-HCl (pH 7.6), 1 mmol L⁻¹ EGTA, 1 mmol L⁻¹ dithiothreitol, and
31
32 1 mmol L⁻¹ phenylmethylsulfonyl fluoride). The activity of P-type ATPase was determined
33
34 by the release of phosphate during P_i or ATP hydrolysis according to the previous method.⁴⁸
35
36
37 The determination was performed using the reaction medium of 20 mmol L⁻¹ Mops-BTP (pH
38
39 8.0), 50 mmol L⁻¹ MgSO₄, 200 μmol L⁻¹ Na₂MoO₄, 1 mmol L⁻¹ ATP. One U of P-type
40
41 ATPase activity was expressed as μmol Pi mg⁻¹ protein h⁻¹.
42
43
44
45
46
47
48
49

50 MTs concentration was measured according to the published study.⁴⁹ Fresh wheat leaf
51
52 tissues (1 g) were ground into homogenate with Tris-HCl buffer (0.1 mol L⁻¹, pH 8.6), and
53
54 then the homogenate was allowed to rest for 24 h. After centrifugation at 10,000 g for 10 min
55
56 at 4 °C, the supernatant was collected, and heated in a water bath for 3 min at 90 °C.
57
58
59
60

1
2
3
4 Subsequently, the cooled solution was centrifuged at 10,000 g for 15 min at 4 °C. A three
5
6 times volume of absolute ethanol was added to the collected supernatant, and then the mixed
7
8 solution was stored at -20 °C for 24 h. After that, the solution was centrifuged at 10,000 g for
9
10 15 min at 4 °C, and the supernatant was discarded. After adding 5 mL Tris-HCl buffer (0.1
11
12 mol L⁻¹, pH 8.6) to dissolve the precipitate, the solution was again centrifuged at 10,000 g
13
14 for 10 min at 4 °C and the MTs concentration was determined. First, 0.5 mL 5 μmol L⁻¹
15
16 DTNB (5,5'-dithiobis-(2-nitrobenzoic acid)) solution and 2.5 mL Tris-HCl buffer (0.1 mol
17
18 L⁻¹, pH 8.6) were added to 1 mL of the MTs supernatant, and the absorbance value was
19
20 measured at 412 nm. MTs concentration (μmol·g⁻¹ fresh weight) was calculated according
21
22 to a constructed standard curve (Fig. S10†).
23
24
25
26
27
28
29
30
31

32 **Statistical analysis**

33
34 A one-way analysis of variance (ANOVA) and *Duncan's* test was performed to analyze the
35
36 data. Statistical analyses were carried out using the statistical analysis software (Version 9.2,
37
38 SAS Institute Cary, NC, 2010). All data were expressed as mean ± standard deviation (SD).
39
40
41
42
43 Statistical significance was based on p<0.05.
44
45
46
47
48
49

50 **Results and discussion**

51 **Characterization of ZnO NPs and FITC-ZnO NPs**

52
53
54 The zeta potential, particle size and dissolution of ZnO NPs and FITC-ZnO NPs were
55
56 measured in deionized water at the same concentration. The average hydrodynamic particle
57
58
59
60

1
2
3
4 diameters of ZnO NPs and FITC-ZnO NPs were statistically equivalent at 341.2 and 363.9
5
6 nm, respectively (Table S1†). Similarly, no significant differences were found in zeta
7
8 potential (-16.3 and -19.4 mV), suspension pH (7.56 and 7.50) and conductivity (1.70 and
9
10 1.67 $\mu\text{s cm}^{-1}$) for the unlabeled and labeled ZnO NPs suspensions, respectively. The time-
11
12 dependent dissolution of ZnO NPs and FITC-ZnO NPs in deionized water was measured (Fig.
13
14 S1†). The concentration of released Zn^{2+} reached a maximum of 1.31 and 1.22 mg L^{-1} at 24
15
16 h for ZnO NPs and FITC-ZnO NPs, respectively. No significant difference between the two
17
18 treatments was observed at the same time point. These results indicate that FITC has no
19
20 apparent influence on ZnO NPs hydrodynamic diameter and zeta potential in deionized water.
21
22 Our results (Fig. S2†) displayed that the FITC could stay on the NPs over 24 h at different
23
24 pH solutions (pH 5.8 and 7.0). As such, FITC is a suitable label to investigate ZnO NPs
25
26 detection, absorption and localization in wheat leaves.
27
28
29
30
31
32
33
34
35
36
37

38 **Absorption pathway of ZnO NPs in crossing the leaf epidermis**

39
40 We hypothesize that the absorption of NPs by plant leaves occurs primarily through the
41
42 stomata; the stomatal pore diameter varies with species and other factors but is approximately
43
44 3.5-100 μm .⁵⁰ It is well known that abscisic acid (ABA) amendment can affect the stomata
45
46 aperture.^{51,52} To evaluate our hypothesis, an ABA solution (100 $\mu\text{mol L}^{-1}$, estimated volume:
47
48 40 μL per exposed leaf) was sprayed on wheat leaves to induce stomatal closure. Treatment
49
50 of 100 $\mu\text{mol L}^{-1}$ ABA significantly decreased the stomatal aperture of wheat leaves by 39.4%
51
52 compared to controls (Fig. 1).
53
54
55
56
57

58 To investigate the main route of ZnO NPs absorption and translocation, an experiment
59
60

1
2
3
4 was designed as follows. The control and treated groups were sprayed with deionized water
5
6 and $100 \mu\text{mol L}^{-1}$ ABA solution ($40 \mu\text{L}$ per exposed leaf) on the leaves, respectively. After
7
8
9 2 h, $100 \mu\text{mol L}^{-1}$ FITC-ZnO NPs suspension ($40 \mu\text{L}$ per exposed leaf) was sprayed on
10
11 wheat leaves in all groups. All samples were observed with a Leica confocal laser scanning
12
13 microscope. Previous studies have displayed that the FITC labelling method is mature and
14
15 reliable, and has no significant effects on the behavior of NPs in plant leaves.^{53,54} Although
16
17 leaf tissues auto-fluoresce, the Leica confocal laser scanning microscope is able to eliminate
18
19 it and readily discern the guard cells. With consideration of a previous study³⁵ and our
20
21 experiments (Fig. S3[†]), FITC molecules alone do not result in a cellular staining profile.
22
23 Hence, the green fluorescence was all from the FITC-ZnO NPs. Fig. 2 shows the confocal
24
25 images of ZnO NPs treated wheat leaves with or without ABA treatment at different time
26
27 points over 24 h. The chloroplast emits red fluorescence under the condition of green
28
29 excitation and can serve as a reference to identify the penetration depth (Z dimension) of
30
31 ZnO NPs (green fluorescence) in the wheat leaf tissues. Due to the effect of ABA on
32
33 reducing the stomatal aperture, the amount of ZnO NPs in the ABA-treated groups was
34
35 notably less than the controls at equivalent time points. This demonstrates that there is a
36
37 positive correlation between stomatal aperture and the amount of ZnO NPs entry. From the
38
39 images, it is clear that the ZnO NPs initially accumulate below the stomata but then begin
40
41 to spread in all directions over time. Most of the particles rapidly accumulate in the space
42
43 between cell walls near the stomata (labeled with yellow boxes and words in Fig. 2),
44
45 suggesting that the mobility of ZnO NPs was limited in the leaf tissues. At 24 h, it is clear
46
47 that just a few ZnO NPs were transported into the cytoplasm. We did not observe the process
48
49
50
51
52
53
54
55
56
57
58
59
60

1
2
3
4 of how they cross the cell wall and enter into the cytoplasm. However, some studies showed
5
6 that NPs can induce new and larger pores in the cell wall, thereby facilitating subsequent
7
8 entry into the cell through this route.^{27,55}
9
10

11
12 No significant differences in transfer rate of nanoparticles were observed after leaf wax
13
14 was removed by 60% in mass,⁵⁶ and the cuticle could encapsulate the nanoparticles.⁵⁷ This
15
16 suggests that nanoparticle entry into leaf epidermis through the cuticle is likely highly
17
18 restricted. For the undissolved nanoparticles such as Au NPs, stomata are an important
19
20 pathway to enter into plant leaves.⁵⁸ Avellan et al.⁵⁹ found that polyvinylpyrrolidone-coated
21
22 Au NPs could be absorbed by cuticle, but the entry of negatively charged citrate-coated Au
23
24 NPs was observed through stomata. It seems that the properties of the particles have an
25
26 important effect on the stomatal absorption pathway. When the ZnO NPs aqueous
27
28 suspension was applied on the leaf surface, a hydraulic connection between the inside and
29
30 outside of stoma was easily established by a thin film of water, and it enhanced the transfer
31
32 of ZnO NPs in the suspension.^{29,60,61} Hence, the negatively charged ZnO NPs could be
33
34 transported through stomatal pathway. Given this and our current findings, the stomatal
35
36 pathway appears to be the main route for ZnO NPs absorption by wheat leaves.
37
38
39
40
41
42
43
44
45
46
47

48 **Translocation and distribution of Zn in leaf mesophyll**

49
50 The distribution of Zn in wheat leaf tissue vertical cross-sections was determined by an ultra-
51
52 high resolution (1.0 nm) scanning electron microscopy (SEM). Due to the low level, no Zn
53
54 element was found in the reference (wheat leaves treated without ZnO NPs and ZnSO₄) by
55
56 SEM elemental mapping (Fig. S4†). The concentrations of both ZnO NPs and ZnSO₄ were
57
58
59
60

1
2
3
4 increased to 1 mmol L⁻¹ to facilitate detection; a number of studies have reported no
5
6 phytotoxicity in wheat at this concentration.^{18,58} From the SEM elemental mapping (Fig. 3),
7
8 Zn is clearly evident in all treated sample cross-sections, and the concentrations of Zn in the
9
10 tissues of both treatments increases over time. Interestingly, Zn occurred at low amounts in
11
12 the cross-sections of the NPs treatments at 48 h; there was greater occurrence in the leaf
13
14 tissues treated with ZnSO₄. In addition, the distribution of Zn in wheat leaves exposed to
15
16 ZnO NPs was heterogeneous relative to the more homogeneous distribution evident with the
17
18 salt exposure at 48 h. Specifically, most Zn was distributed in the upper and lower mesophyll
19
20 tissues in ZnO NPs treatment, and the tissue close to the lower epidermis had higher Zn
21
22 amounts than did the upper epidermis. In addition, ZnO NPs was present primarily in the
23
24 intercellular space at 24 h combined with the confocal laser scanning microscopy images,
25
26 and then a fraction of the particles diffused to the cytoplasm at 48 h. The salt exposure
27
28 became homogeneously distributed over time. In addition, Zn would likely be non-detectable
29
30 in the control cross-sections.
31
32
33
34
35
36
37
38
39

40
41 There are several possible explanations for the distribution of ZnO NPs in wheat leaf tissue
42
43 cross-sections. It is known that soluble nanomaterials such as ZnO can dissolve on or in plant
44
45 tissues over time.³¹ The in planta translocation of nanoparticles is primarily affected by both
46
47 charge (for undissolved particles, a corona will form and the protein or biomolecular corona
48
49 can impact transport as much as or perhaps more than size)⁶² and particle size; importantly,
50
51 the particles need to traverse a series of barriers with specific size exclusion limits.³¹
52
53
54

55
56 Accordingly, after crossing the leaf epidermis, ZnO NPs would be restricted by the cell
57
58 wall, likely accumulating in the intercellular space and starting to dissolve. At that same time,
59
60

1
2
3
4 a biomolecular corona will likely continue to form, having unknown impacts on particle fate
5
6 and transport. Important, the SEM elemental mapping indicated that Zn was mainly
7
8 distributed in the upper and lower mesophyll tissues for ZnO NPs treatment. However, the
9
10 spread of Zn was most in the middle of leaf tissue vertical cross-section for ZnSO₄ treatment
11
12 at 24 h. Combined with the results (Fig. S5†), one probable reason for this phenomenon is
13
14 that salts could not be limited by cell wall and their diffusion in apoplast and cytoplasm
15
16 occurs more quickly than nanoparticles. Because the lower epidermis has more stomata,⁶³ Zn
17
18 concentration in the tissues close to lower epidermis is greater than that in the upper
19
20 epidermis. As time passes, the quantity of ZnO NPs in the leaf tissues increases, as does the
21
22 amount specifically in both apoplast and cytoplasm. Hence, the distribution of Zn in leaf
23
24 tissues becomes more homogeneous over time.
25
26
27
28
29
30
31
32
33
34

35 **Zn concentrations in the apoplast and cytoplasm of mesophyll cells**

36
37 After accumulating in the apoplast, nanoparticles could also begin to dissolve. As shown in
38
39 Fig. 4, the concentration of Zn in the apoplast increased over time in all treatments (ZnO NPs
40
41 alone or with ABA) compared to the control and sole abscisic acid (ABA) (Fig. 4A). With
42
43 co-treatment of 100 μmol L⁻¹ ZnO NPs and 100 μmol L⁻¹ ABA on wheat leaves, the Zn²⁺
44
45 concentration was significantly reduced by 33.2% compared to the NP-alone (100 μmol L⁻¹)
46
47 treatment. No significant difference was found between the control and ABA treatments. The
48
49 cytoplasmic Zn²⁺ concentrations in both the ZnO NPs and ZnO NPs plus ABA treatments
50
51 have similar trend; initially high levels that then gradually decline over time. The Zn²⁺
52
53 concentrations reached the highest value at 4 h in ZnO NPs alone (11.31 mg kg⁻¹ FW) and
54
55
56
57
58
59
60

1
2
3
4 combined ABA treatments ($9.63 \text{ mg kg}^{-1} \text{ FW}$), respectively. However, concentrations in the
5
6 cytoplasm then decreased over time by an average of 8.3%. As shown in Fig. 4C, the Zn^{2+}
7
8 concentrations in intact wheat leaves (apoplast and cytoplasm) was similar for the ZnO NP-
9
10 alone and combined ABA treatment; levels rose for the first 4 hours but were then stable for
11
12 the remainder of the exposure. Importantly, ABA treatment reduced total Zn^{2+} concentration
13
14 in wheat leaves by up to 23%.
15
16
17
18

19 Foliar application of ZnO NPs can significantly increase Zn concentration in plants;²⁰ ZnO
20
21 NPs are known to be both soluble in plant tissues and to be transformed into other ionic forms
22
23 that may be either bound or free fractions.³⁵ In our study, the Zn concentrations of leaf tissues
24
25 in the NP treatments increased to varying degrees. Although ZnO NPs (particles or their
26
27 aggregation) are smaller than the stomatal aperture, the absorption amount of ZnO NPs will
28
29 be affected by the changes of stomatal aperture as a function of environmental conditions
30
31 and internal physiology (i.e. stomatal dynamical open and close). It means that the flux would
32
33 be affected by the changes in stomatal aperture. Our results displayed that total Zn
34
35 concentration (apoplastic and cytoplasmic Zn) was proportional to the stomatal aperture. Zn
36
37 concentration in apoplast was more significantly affected by the changes of stomatal aperture
38
39 than that in cytoplasm. There are several possible explanations for this result. For example,
40
41 the cell wall may have blocked NPs passage, leading to the accumulation of ZnO NPs in the
42
43 apoplast. The pH of apoplastic fluid is about 5.8,⁶⁴ which is significantly lower than that of
44
45 cytoplasm (about pH 7.5). This pH difference could lead directly to greater ion dissolution
46
47 from the ZnO NPs (Fig. S6†) into the apoplast.⁶⁵
48
49
50
51
52
53
54
55
56
57

58 The P-type ATPase can transport a variety of cations such as Cd^{2+} , Cu^{2+} and Zn^{2+} across
59
60

1
2
3
4 membranes.⁶⁶ These transporters can be found in the membrane system of cells and are
5
6 known to remove toxic or excess metal ions from the cytoplasm. For example, the expression
7
8 of the H⁺-ATPase gene (*HAI*) can be induced by metal cations such as Pb²⁺, Cd²⁺ and
9
10 Zn²⁺.^{67,68} Metallothioneins (MTs) are widely distributed among animal and plant cells and
11
12 have a strong affinity for binding heavy metals.⁶⁹ This protein can bind to metals through a
13
14 thiol group of cysteine and exerts an important role in heavy metal homeostasis within plant
15
16 cells.⁷⁰ To better understand the translocation of ZnO NPs from the apoplast to the cytoplasm,
17
18 we measured the relative expression of *HAI* and *Metallothionein (class II)*, enzyme activity
19
20 of P-type ATPase, and the concentrations of MTs and Zn at five time points (2, 4, 8, 16 and
21
22 24 h) in three treatments (control, 100 μmol L⁻¹ ZnSO₄ and ZnO NPs). The expression level
23
24 of *HAI* in the ZnSO₄ treatment was significantly up-regulated at the first two time points,
25
26 and declined after 4 h (Fig. 5A). Unlike salt exposure, in the ZnO NPs treatment the *HAI*
27
28 expression level was most significantly up-regulated only at 8 h. When considering P-type
29
30 ATPase activity within the leaf tissues (Fig. 5C), there are no significant differences among
31
32 the three treatments during the first 8 h. However, enzyme activity levels increased at 16 h
33
34 and 24 h for both the ZnSO₄ and ZnO NPs treatments compared to the controls; there was no
35
36 difference between the particle types. For *Metallothionein (class II)* expression (Fig. 5B),
37
38 ZnO NPs and ZnSO₄ treatments exhibited similar trends; significant up-regulation was
39
40 evident at 4 h, but the expression declined over time. Importantly, overall expression levels
41
42 for *Metallothionein (class II)* were significantly greater for the ZnSO₄ treatment as compared
43
44 to ZnO NPs at most time points. Fig. 5D shows that MTs concentration was increased in the
45
46 two Zn treatments at 8, 16 and 24 h compared to the control; levels were highest at 8 h and
47
48
49
50
51
52
53
54
55
56
57
58
59
60

1
2
3
4 declined steadily thereafter. Through the results (Fig. S5†) Zn concentration in ZnO NPs
5
6 treatment was higher than that in ZnSO₄ treatment in apoplast, and an opposite result was
7
8 shown in cytoplasm.
9
10

11 Although plants are known to absorb Zn cations by a foliar pathway, the mechanism of
12 ZnO NPs absorption is not known.⁷¹ The surface properties of plant leaves such as stomatal
13
14 number and diameter, as well as cuticle thickness and chemical composition, control the
15
16 absorption of Zn.⁷² When a ZnSO₄ solution is foliarly applied, Zn²⁺ may be absorbed through
17
18 stomata and/or cuticle, with transport into leaf apoplast. During this process, part of Zn
19
20 cations will be absorbed by mesophyll cells into leaf cytoplasm, with additional Zn ions being
21
22 transported through the extracellular apoplastic route.⁷ However, the ZnO NPs suspension
23
24 will result in a different behavior on and in the plant leaves. The differences between the two
25
26 treatments (Fig. S5†) indicate that ZnO NPs are not readily absorbed by the cells. This is
27
28 likely due to the barrier function of cell wall, which results in the accumulation of ZnO NPs
29
30 in the apoplast. Conversely, the ZnSO₄ solution has much greater Zn cations which easily
31
32 cross the cell wall and are absorbed by mesophyll cells. Consequently, the ZnSO₄ exposure
33
34 leads to greater Zn in the cytoplasm as compared to the nanoparticle treatment. This
35
36 phenomenon is also supported by the gene expression data for *HAI* and *Metallothionein*
37
38 (*class II*) (Fig. 5). We think that the reason for delayed expression of *HAI* may be due to the
39
40 dissolution process of ZnO NPs in the apoplastic fluid. Because it should take some time to
41
42 release Zn ions from ZnO NPs, the genetic response would be delayed and slower.
43
44 Conversely, ZnSO₄ could release Zn ions very quickly and the released Zn ions could rapidly
45
46 be absorbed by cells. Because of the above findings, we speculated that ZnO NPs accumulate
47
48
49
50
51
52
53
54
55
56
57
58
59
60

1
2
3
4 in leaf apoplast after entry through the stomata, and then partially dissolve over time to
5
6 release Zn^{2+} that may be absorbed by the mesophyll cells or accumulate in leaf cytoplasm.
7
8
9

10 11 12 13 14 **Conclusions**

15
16 ZnO NPs are a representative soluble nanoparticle readily biotransformed both on and in
17
18 plants. Our results indicate that the main route for ZnO NPs entry to the wheat leaf epidermis
19
20 after foliar spraying is through the stomata (Fig. 6). ZnO NPs largely accumulate below the
21
22 stomata and then move through the apoplast over time. During transport, a fraction of the
23
24 ZnO NPs will dissolve in the apoplast and release Zn cations that are absorbed by mesophyll
25
26 cells. The undissolved ZnO NPs are also partly transferred into the cells. Our study mainly
27
28 focused on the initial entry and distribution in a short time. Over weeks and months of
29
30 subsequent plant growth, dynamic transformation processes will continue to impact particle
31
32 fate in the tissues. These findings will help us to understand the ZnO NPs absorption and
33
34 distribution in plant leaves, including key differences from more traditional forms of the
35
36 nutrient, and will provide valuable information to guide the sustainable use of ZnO NPs and
37
38 potentially other soluble NPs in agriculture.
39
40
41
42
43
44
45
46
47
48
49
50
51
52

53 **Conflict of interest**

54
55
56 The authors declare no conflict of interest.
57
58
59
60

Acknowledgments

This work was supported by the National Natural Science Foundation of China (31770546, 31370521). BX thanks UMass Amherst Conti fellowship (2019-2020) and JCW acknowledges USDA Hatch CONH 00147. Jiahui Zhu thanks the China Scholarship Council (CSC) for the financial support to study at the University of Massachusetts, Amherst.

References

- 1 M. Kah, N. Tufenkji and J. C. White, Nano-enabled strategies to enhance crop nutrition and protection, *Nat. Nanotechnol.*, 2019, **14**, 532-540.
- 2 E. Corradini, M. R. de Moura and L. H. C. Mattoso, A preliminary study of the incorporation of NPK fertilizer into chitosan nanoparticles, *Express Polym. Lett.*, 2010, **4**, 509-515.
- 3 S. Sharma, S. Singh, A. K. Ganguli and V. Shanmugam, Anti-drift nano-stickers made of graphene oxide for targeted pesticide delivery and crop pest control, *Carbon*, 2017, **115**, 781-790.
- 4 Q. Liu, F. Li, H. Lu, M. Li, J. Liu, S. Zhang, Q. Sun and L. Xiong, Enhanced dispersion stability and heavy metal ion adsorption capability of oxidized starch nanoparticles, *Food Chem.*, 2018, **242**, 256-263.
- 5 C. Larue, J. Laurette, N. Herlin-Boime, H. Khodja, B. Fayard, A. M. Flank, F. Brisset and M. Carriere, Accumulation, translocation and impact of TiO₂ nanoparticles in

- 1
2
3
4 Wheat (*Triticum aestivum* spp.): influence of diameter and crystal phase, *Sci. Total*
5
6 *Environ.*, 2012, **431**, 197-208.
7
8
- 9 6 C. O. Dimkpa, J. C. White, W. H. Elmer and J. Gardea-Torresdey, Nanoparticle and
10
11 ionic Zn promote nutrient loading of sorghum grain under low NPK fertilization, *J.*
12
13 *Agr. Food Chem.*, 2017, **65**, 8552-8559.
14
15
- 16 7 V. Kumar, P. Guleria, V. Kumar and S. K. Yadav, Gold nanoparticle exposure
17
18 induces growth and yield enhancement in *Arabidopsis thaliana*, *Sci. Total Environ.*,
19
20 2013, **461-462**, 462-468.
21
22
23
- 24 8 L. V. Subbaiah, T. N. Prasad, T. G. Krishna, P. Sudhakar, B. R. Reddy and T. Pradeep,
25
26 Novel effects of nanoparticulate delivery of zinc on growth, productivity, and zinc
27
28 biofortification in maize (*Zea mays* L.), *J. Agr. Food Chem.*, 2016, **64**, 3778-3788.
29
30
31
- 32 9 T. L. Read, C. L. Doolette, T. Cresswell, N. R. Howell, R. Aughterson, I.
33
34 Karatchevtseva, E. Donner, P. M. Kopittke, J. K. Schjoerring and E. Lombi,
35
36 Investigating the foliar uptake of zinc from conventional and nano-formulations: a
37
38 methodological study, *Environ Chem*, 2019, **16**, 459-469.
39
40
41
- 42 10 A. Rehman, M. Farooq, R. Ahmad and S. M. A. Basra, Seed priming with zinc
43
44 improves the germination and early seedling growth of wheat, *Seed Sci. Technol.*,
45
46 2015, **43**, 262-268.
47
48
49
- 50 11 A. Rehman and M. Farooq, Zinc seed coating improves the growth, grain yield and
51
52 grain biofortification of bread wheat, *Acta Physiol. Plant.*, 2016, **38**,
53
54 DOI:10.1007/s11738-11016-12250-11733
55
56
57
- 58 12 K. Bharti, N. Pandey, D. Shankhdhar, P. C. Srivastava and S. C. Shankhdhar, Effect
59
60

- 1
2
3
4 of exogenous zinc supply on photosynthetic rate, chlorophyll content and some
5
6 growth parameters in different wheat genotypes, *Cereal Res. Commun.*, 2014, **42**,
7
8 589-600.
9
10
11
12 13 D. Singh, S. Yadav and N. Nautiyal, Evaluation of growth responses in wheat as
14 affected by the application of zinc and boron to a soil deficient in available zinc and
15 boron, *Commun. Soil Sci. Plant*, 2014, **45**, 765-776.
16
17
18
19 14 C. Q. Zou, Y. Q. Zhang, A. Rashid, H. Ram, E. Savasli, R. Z. Arisoy, I. Ortiz-
20 Monasterio, S. Simunji, Z. H. Wang, V. Sohu, M. Hassan, Y. Kaya, O. Onder, O.
21 Lungu, M. Y. Mujahid, A. K. Joshi, Y. Zelenskiy, F. S. Zhang and I. Cakmak,
22 Biofortification of wheat with zinc through zinc fertilization in seven countries, *Plant*
23 *Soil*, 2012, **361**, 119-130.
24
25
26
27
28
29
30
31
32 15 G. M. Manzeke, F. Mtambanengwe, H. Nezomba and P. Mapfumo, Zinc fertilization
33 influence on maize productivity and grain nutritional quality under integrated soil
34 fertility management in zimbabwe, *Field Crop. Res.*, 2014, **166**, 128-136.
35
36
37
38
39
40 16 J. Wang, H. Mao, H. Zhao, D. Huang and Z. Wang, Different increases in maize and
41 wheat grain zinc concentrations caused by soil and foliar applications of zinc in loess
42 plateau, China, *Field Crop. Res.*, 2012, **135**, 89-96.
43
44
45
46
47
48 17 T. N. M. da Cruz, S. M. Savassa, M. H. F. Gomes, E. S. Rodrigues, N. M. Duran, E.
49 de Almeida, A. P. Martinelli and H. W. P. de Carvalho, Shedding light on the
50 mechanisms of absorption and transport of ZnO nanoparticles by plants *via in vivo*
51 X-ray spectroscopy, *Environ. Sci.: Nano*, 2017, **4**, 2367-2376.
52
53
54
55
56
57
58 18 T. Zhang, H. Sun, Z. Lv, L. Cui, H. Mao and P. M. Kopittke, Using synchrotron-
59
60

- 1
2
3
4 based approaches to examine the foliar application of ZnSO₄ and ZnO nanoparticles
5
6 for field-grown winter wheat, *J. Agr. Food Chem.*, 2018, **66**, 2572-2579.
7
8
- 9 19 L. Rossi, L. N. Fedenia, H. Sharifan, X. Ma and L. Lombardini, Effects of foliar
10 application of zinc sulfate and zinc nanoparticles in coffee (*Coffea arabica* L.) plants,
11
12 *Plant Physiol. Biochem.*, 2019, **135**, 160-166.
13
14
- 15 20 T. N. V. K. V. Prasad, P. Sudhakar, Y. Sreenivasulu, P. Latha, V. Munaswamy, K.
16
17 R. Reddy, T. S. Sreeprasad, P. R. Sajanlal and T. Pradeep, Effect of nanoscale zinc
18
19 oxide particles on the germination, growth and yield of peanut, *J. Plant Nutr.*, 2012,
20
21
22 **35**, 905-927.
23
24
25
- 26 21 N. Milani, M. J. McLaughlin, S. P. Stacey, J. K. Kirby, G. M. Hettiarachchi, D. G.
27
28 Beak and G. Cornelis, Dissolution kinetics of macronutrient fertilizers coated with
29
30 manufactured zinc oxide nanoparticles, *J. Agric. Food Chem.*, 2012, **60**, 3991-3998.
31
32
33
- 34 22 C. M. D. Monreal, M.; Mallubhotla, S. C.; Bindraban, P. S.; Dimkpa, C.,
35
36 Nanotechnologies for increasing the crop use efficiency of fertilizer-micronutrients,
37
38 *Biol. Fertil. Soils*, 2015, **52**, 423-437.
39
40
41
- 42 23 M. El-Kereti, S. El-feky, M. Khater, Y. Osman and E. El-sheibini, ZnO nanofertilizer
43
44 and He Ne laser irradiation for promoting growth and yield of sweet basil plant,
45
46
47 *Recent Pat. Food Nutr. Agr.*, 2014, **5**, 169-181.
48
49
- 50 24 R. Raliya and J. C. Tarafdar, ZnO nanoparticle biosynthesis and its effect on
51
52 phosphorous-mobilizing enzyme secretion and gum contents in clusterbean
53
54 (*Cyamopsis tetragonoloba* L.), *Agr. Res.*, 2013, **2**, 48-57.
55
56
57
- 58 25 P. Zhao, L. Cao, D. Ma, Z. Zhou, Q. Huang and C. Pan, Translocation, distribution
59
60

- 1
2
3
4 and degradation of prochloraz-loaded mesoporous silica nanoparticles in cucumber
5
6 plants, *Nanoscale*, 2018, **10**, 1798-1806.
7
8
- 9 26 S. Lin, J. Reppert, Q. Hu, J. S. Hudson, M. L. Reid, T. A. Ratnikova, A. M. Rao, H.
10
11 Luo and P. C. Ke, Uptake, translocation, and transmission of carbon nanomaterials
12
13 in rice plants, *Small*, 2009, DOI: 10.1002/sml.200801556, 1128-1132.
14
15
- 16 27 J. Kurepa, T. Paunesku, S. Vogt, H. Arora, B. M. Rabatic, J. Lu, M. B. Wanzer, G.
17
18 E. Woloschak and J. A. Smalle, Uptake and distribution of ultrasmall anatase TiO₂
19
20 alizarin red S nanoconjugates in *Arabidopsis thaliana*, *Nano Lett.*, 2010, **10**, 2296-
21
22 2302.
23
24
25
- 26 28 T. Xiong, C. Dumat, V. Dappe, H. Vezin, E. Schreck, M. Shahid, A. Pierart and S.
27
28 Sobanska, Copper oxide nanoparticle foliar uptake, phytotoxicity, and consequences
29
30 for sustainable urban agriculture, *Environ. Sci. Technol.*, 2017, **51**, 5242-5251.
31
32
33
- 34 29 T. Eichert, A. Kurtz, U. Steiner and H. E. Goldbach, Size exclusion limits and lateral
35
36 heterogeneity of the stomatal foliar uptake pathway for aqueous solutes and water-
37
38 suspended nanoparticles, *Physiol. Plant.*, 2008, **134**, 151-160.
39
40
41
- 42 30 M. H. F. Gomes, B. A. Machado, E. S. Rodrigues, G. S. Montanha, M. L. Rossi, R.
43
44 Otto, F. S. Linhares and C. H. W. P., *In vivo* evaluation of Zn foliar uptake and
45
46 transport in soybean using X-Ray absorption and fluorescence spectroscopy, *J. Agric.*
47
48 *Food Chem.*, 2019, **67**, 12172-12181.
49
50
51
- 52 31 P. Wang, E. Lombi, F. J. Zhao and P. M. Kopittke, Nanotechnology: a new
53
54 opportunity in plant sciences, *Trends Plant Sci.*, 2016, **21**, 699-712.
55
56
57
- 58 32 C. Li, P. Wang, E. Lombi, M. Cheng, C. Tang, D. L. Howard, N. W. Menzies and P.
59
60

- 1
2
3
4 M. Kopittke, Absorption of foliar-applied Zn fertilizers by trichomes in soybean and
5
6 tomato, *J. Exp. Bot.*, 2018, **69**, 2717-2729.
7
8
- 9 33 S. G. Wu, H. Li, J. Head, D. Chen, I. Kong and Y. J. Tang, Phytotoxicity of metal
10
11 oxide nanoparticles is related to both dissolved metals ions and adsorption of particles
12
13 on seed surfaces, *J. Pet. Environ. Biotechnol.*, 2012, **03**, DOI: 10.4172/2157-
14
15 7463.1000126.
16
17
- 18 34 F. Schwabe, R. Schulin, P. Rupper, A. Rotzetter, W. Stark and B. Nowack,
19
20
21 Dissolution and transformation of cerium oxide nanoparticles in plant growth media,
22
23
24 *J. Nanopart. Res.*, 2014, **16**, DOI: 10.1007/s11051-11014-12668-11058.
25
26
- 27 35 T. Xia, M. Kovochich, M. Liong, L. Mädler, B. Gilbert, H. Shi, J. I. Yeh, J. I. Zink
28
29
30 and A. E. Nel, Comparison of the mechanism of toxicity of zinc oxide and cerium
31
32
33 oxide nanoparticles based on dissolution and oxidative stress properties, *ACS Nano*,
34
35
36 2008, **2**, 2121-2134.
37
- 38 36 J. Zhu, Z. Zou, Y. Shen, J. Li, S. Shi, S. Han and X. Zhan, Increased ZnO nanoparticle
39
40
41 toxicity to wheat upon co-exposure to phenanthrene, *Environ. Pollut.*, 2019, **247**,
42
43
44 108-117.
45
- 46 37 R. Ma, C. Levard, F. M. Michel, G. E. Brown, Jr.; and G. V. Lowry, Sulfidation
47
48
49 mechanism for zinc oxide nanoparticles and the effect of sulfidation on their
50
51
52 solubility, *Environ. Sci. Technol.*, 2013, **47**, 2527-2534.
53
- 54 38 Y. Shang, C. Dai, M. M. Lee, J. M. Kwak and K. H. Nam, BRI1-associated receptor
55
56
57 kinase 1 regulates guard cell ABA signaling mediated by open stomata 1 in
58
59
60 *Arabidopsis*, *Mol. Plant*, 2016, **9**, 447-460.

- 1
2
3
4 39 A. O’Carrigan, E. Hinde, N. Lu, X. Xu, H. Duan, G. Huang, M. Mak, B. Bellotti and
5
6 Z. Chen, Effects of light irradiance on stomatal regulation and growth of tomato,
7
8 *Environ. Exp. Bot.*, 2014, **98**, 65-73.
9
10
11 40 H. Wu, N. Tito and J. P. Giraldo, Anionic cerium oxide nanoparticles protect plant
12
13 photosynthesis from abiotic stress by scavenging reactive oxygen species, *ACS Nano*,
14
15 2017, **11**, 11283-11297.
16
17
18 41 H. Zhang, L. Lu, X. Zhao, S. Zhao, X. Gu, W. Du, H. Wei, R. Ji and L. Zhao,
19
20 Metabolomics reveals the "invisible" responses of spinach plants exposed to CeO₂
21
22 nanoparticles, *Environ. Sci. Technol.*, 2019, **53**, 6007-6017.
23
24
25
26 42 N. T. Dinh, D. T. Vu, D. Mulligan and A. V. Nguyen, Accumulation and distribution
27
28 of zinc in the leaves and roots of the hyperaccumulator *Noccaea caerulescens*,
29
30 *Environ. Exp. Bot.*, 2015, **110**, 85-95.
31
32
33
34 43 J. Ye, C. Yan, J. Liu, H. Lu, T. Liu and Z. Song, Effects of silicon on the distribution
35
36 of cadmium compartmentation in root tips of *Kandelia obovata* (S., L.) Yong,
37
38 *Environ. Pollut.*, 2012, **162**, 369-373.
39
40
41
42 44 X. Zhan, M. Zhu, Y. Shen, L. Yue, J. Li, J. L. Gardea-Torresdey and G. Xu,
43
44 Apoplastic and symplastic uptake of phenanthrene in wheat roots, *Environ. Pollut.*,
45
46 2018, **233**, 331-339.
47
48
49
50 45 Z. Wu, F. Wang, S. Liu, Y. Du, F. Li, R. Du, D. Wen and J. Zhao, Comparative
51
52 responses to silicon and selenium in relation to cadmium uptake, compartmentation
53
54 in roots, and xylem transport in flowering Chinese cabbage (*Brassica campestris* L.
55
56 ssp. *chinensis* var. *utilis*) under cadmium stress, *Environ. Exp. Bot.*, 2016, **131**, 173-
57
58
59
60

- 1
2
3
4 180.
5
6
7 46 J. Li, L. Yue, Y. Shen, Y. Sheng, X. Zhan, G. Xu and B. Xing, Phenanthrene-
8
9 responsive microRNAs and their targets in wheat roots, *Chemosphere*, 2017, **186**,
10
11 588-598.
12
13
14 47 X. Yin, X. Liang, R. Zhang, L. Yu, G. Xu, Q. Zhou and X. Zhan, Impact of
15
16 phenanthrene exposure on activities of nitrate reductase, phosphoenolpyruvate
17
18 carboxylase, vacuolar H⁺-pyrophosphatase and plasma membrane H⁺-ATPase in
19
20 roots of soybean, wheat and carrot, *Environ. Exp. Bot.*, 2015, **113**, 59-66.
21
22
23
24 48 J. Paez-Valencia, J. Sanchez-Lares, E. Marsh, L. T. Dorneles, M. P. Santos, D.
25
26 Sanchez, A. Winter, S. Murphy, J. Cox and M. Trzaska, Enhanced proton
27
28 translocating tyrophosphatase activity improves nitrogen use efficiency in romaine
29
30 lettuce, *Plant Physiol.*, 2013, **161**, 1557-1569.
31
32
33
34
35 49 J. L. Lai and X. G. Luo, High-efficiency antioxidant system, chelating system and
36
37 stress-responsive genes enhance tolerance to cesium ionotoxicity in Indian mustard
38
39 (*Brassica juncea* L.), *Ecotoxicol. Environ. Saf.*, 2019, **181**, 491-498.
40
41
42
43 50 R. Raliya, C. Franke, S. Chavalmane, R. Nair, N. Reed and P. Biswas, Quantitative
44
45 understanding of nanoparticle uptake in watermelon plants, *Front. Plant Sci.*, 2016,
46
47 **7**, DOI: 10.3389/fpls.2016.01288.
48
49
50
51 51 A. Yaaran, B. Negin and M. Moshelion, Role of guard-cell ABA in determining
52
53 steady-state stomatal aperture and prompt vapor-pressure-deficit response, *Plant Sci.*,
54
55 2019, **281**, 31-40.
56
57
58
59 52 M. Haworth, G. Marino, S. L. Cosentino, C. Brunetti, A. De Carlo, G. Avola, E. Riggi,
60

- 1
2
3
4 F. Loreto and M. Centritto, Increased free abscisic acid during drought enhances
5 stomatal sensitivity and modifies stomatal behaviour in fast growing giant reed
6 (*Arundo donax* L.), *Environ. Exp. Bot.*, 2018, **147**, 116-124.
7
8
9
10
11 53 P. Hu, J. An, M. M. Faulkner, H. Wu, Z. Li, X. Tian and J. P. Giraldo, Nanoparticle
12 Charge and Size Control Foliar Delivery Efficiency to Plant Cells and Organelles,
13 *ACS Nano*, 2020, DOI: 10.1021/acsnano.9b09178.
14
15
16
17
18 54 Q. Liu, B. Chen, Q. Wang, X. Shi, Z. Xiao, J. Lin and X. Fang, Carbon Nanotubes as
19 Molecular transporters for walled plant cells, *Nano Lett.*, 2009, **9**, 1007-1010.
20
21
22
23
24 55 S. Eckhardt, P. S. Brunetto, J. Gagnon, M. Priebe, B. Giese and K. M. Fromm,
25 Nanobio silver: its interactions with peptides and bacteria, and its uses in medicine,
26 *Chem. Rev. (Washington, DC, U. S.)*, 2013, **113**, 4708-4754.
27
28
29
30
31 56 V. Dappe, S. Dumez, F. Bernard, B. Hanoune, D. Cuny, C. Dumat and S. Sobanska,
32 The role of epicuticular waxes on foliar metal transfer and phytotoxicity in edible
33 vegetables: case of *Brassica oleracea* species exposed to manufactured particles,
34 *Environ. Sci. Pollut. Res.*, 2019, **26**, 20092-20106.
35
36
37
38
39
40
41 57 A. Saebo, R. Popek, B. Nawrot, H. M. Hanslin, H. Gawronska and S. W. Gawronski,
42 Plant species differences in particulate matter accumulation on leaf surfaces, *Sci.*
43 *Total Environ.*, 2012, **427-428**, 347-354.
44
45
46
47
48
49
50 58 A. Hussain, S. Ali, M. Rizwan, M. Zia Ur Rehman, M. R. Javed, M. Imran, S. A. S.
51 Chatha and R. Nazir, Zinc oxide nanoparticles alter the wheat physiological response
52 and reduce the cadmium uptake by plants, *Environ. Pollut.*, 2018, **242**, 1518-1526.
53
54
55
56
57
58 59 A. Avellan, J. Yun, Y. Zhang, E. Spielman-Sun, J. M. Unrine, J. Thieme, J. Li, E.
60

- 1
2
3
4 Lombi, G. Bland and G. V. Lowry, Nanoparticle size and coating chemistry control
5
6 foliar uptake pathways, translocation, and leaf-to-rhizosphere transport in wheat, *ACS*
7
8 *Nano*, 2019, **13**, 5291-5305.
- 9
10
11 60 T. Eichert and J. Burkhar, Quantification of stomatal uptake of ionic solutes using a
12
13 new model system, *J. Exp. Bot.*, 2001, **52**, 771-781.
- 14
15
16 61 C. Larue, H. Castillo-Michel, S. Sobanska, L. Cecillon, S. Bureau, V. Barthes, L.
17
18 Ouerdane, M. Carriere and G. Sarret, Foliar exposure of the crop *Lactuca sativa* to
19
20 silver nanoparticles: evidence for internalization and changes in Ag speciation, *J.*
21
22 *Hazard Mater.*, 2014, **264**, 98-106.
- 23
24
25
26
27 62 G. Pulido-Reyes, S. M. Briffa, J. Hurtado-Gallego, T. Yudina, F. Leganés, V. Puentes,
28
29 E. Valsami-Jones, R. Rosal and F. Fernández-Piñas, Internalization and toxicological
30
31 mechanisms of uncoated and PVP-coated cerium oxide nanoparticles in the
32
33 freshwater alga *Chlamydomonas reinhardtii*, *Environ. Sci.: Nano*, 2019, **6**, 1959-
34
35 1972.
- 36
37
38
39
40 63 M. Xu, The optimal atmospheric CO₂ concentration for the growth of winter wheat
41
42 (*Triticum aestivum*), *J. Plant Physiol.*, 2015, **184**, 89-97.
- 43
44
45
46 64 V. Gloser, H. Korovetska, A. Martín-Vertedor, M. Hájíčková, Z. Prokop, S.
47
48 Wilkinson and W. Davies, The dynamics of xylem sap pH under drought: a universal
49
50 response in herbs?, *Plant Soil*, 2016, **409**, 259-272.
- 51
52
53
54 65 C. A. David, J. Galceran, C. Rey-Castro, J. Puy, E. Companys, J. Salvador, J. Monné,
55
56 R. Wallace and A. Vakourov, Dissolution kinetics and solubility of ZnO
57
58 nanoparticles followed by AGNES, *J. Phys. Chem. C*, 2012, **116**, 11758-11767.
59
60

- 1
2
3
4 66 A. Moreira, L. A. C. Moraes and A. R. dos Reis, The molecular genetics of zinc
5 uptake and utilization efficiency in crop plants, *Plant Micronutr. Use Effic.*, 2018,
6 DOI: 10.1016/b978-0-12-812104-7.00006-x, 87-108.
7
8
9
10
11 67 S. Bali, V. L. Jamwal, P. Kaur, S. K. Kohli, P. Ohri, S. G. Gandhi, R. Bhardwaj, A.
12 A. Al-Huqail, M. H. Siddiqui and P. Ahmad, Role of P-type ATPase metal
13 transporters and plant immunity induced by jasmonic acid against Lead (Pb) toxicity
14 in tomato, *Ecotoxicol Environ Saf*, 2019, **174**, 283-294.
15
16
17
18
19
20
21 68 N. Satoh-Nagasawa, M. Mori, N. Nakazawa, T. Kawamoto, Y. Nagato, K. Sakurai,
22 H. Takahashi, A. Watanabe and H. Akagi, Mutations in rice (*Oryza Sativa*) heavy
23 metal ATPase 2 (*OsHMA2*) restrict the translocation of zinc and cadmium, *Plant Cell*
24 *Physiol.*, 2012, **53**, 213-224.
25
26
27
28
29
30
31
32 69 M. Tomas, A. Tinti, R. Bofill, M. Capdevila, S. Atrian and A. Torreggiani,
33 Comparative raman study of four plant metallothionein isoforms: insights into their
34 Zn(II) clusters and protein conformations, *J. Inorg. Biochem.*, 2016, **156**, 55-63.
35
36
37
38
39
40 70 S. Clemens, Toxic metal accumulation, responses to exposure and mechanisms of
41 tolerance in plants, *Biochimie*, 2006, **88**, 1707-1719.
42
43
44
45 71 V. Fernandez and P. H. Brown, From plant surface to plant metabolism: the uncertain
46 fate of foliar-applied nutrients, *Front. Plant. Sci.*, 2013, **4**, DOI:
47 10.3389/fpls.2013.00289.
48
49
50
51
52
53 72 T. Eichert and H. E. Goldbach, Equivalent pore radii of hydrophilic foliar uptake
54 routes in stomatous and astomatous leaf surfaces-further evidence for a stomatal
55 pathway, *Physiol. Plant.*, 2008, **132**, 491-502.
56
57
58
59
60

Figures

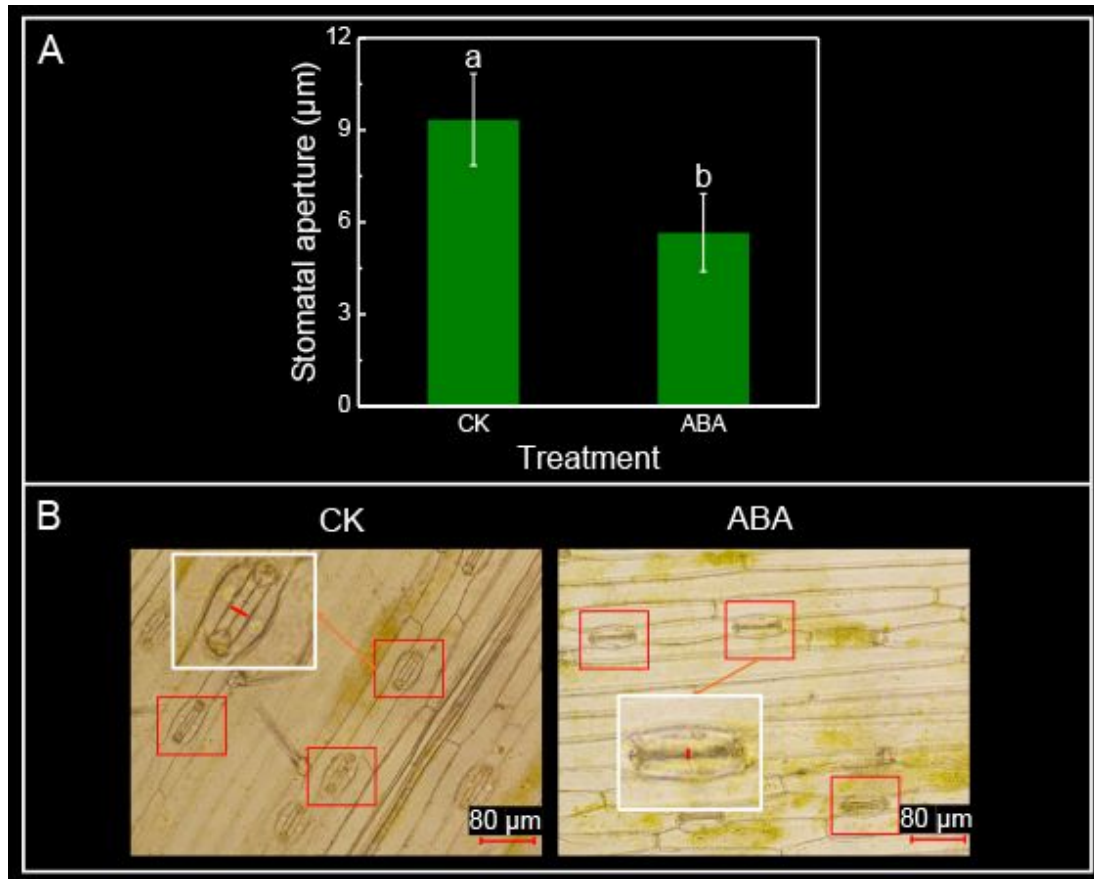


Fig. 1 Stomatal aperture diameter (A) and microscopic images of stomata (B) of wheat lower epidermal treated with or without 100 μmol L⁻¹ abscisic acid (ABA). Each histogram bar represents the mean value of triplicates. Bars are the standard deviation of the mean. Different letters on the top of columns indicate significant difference at $P < 0.05$ according to *Duncan's* test.

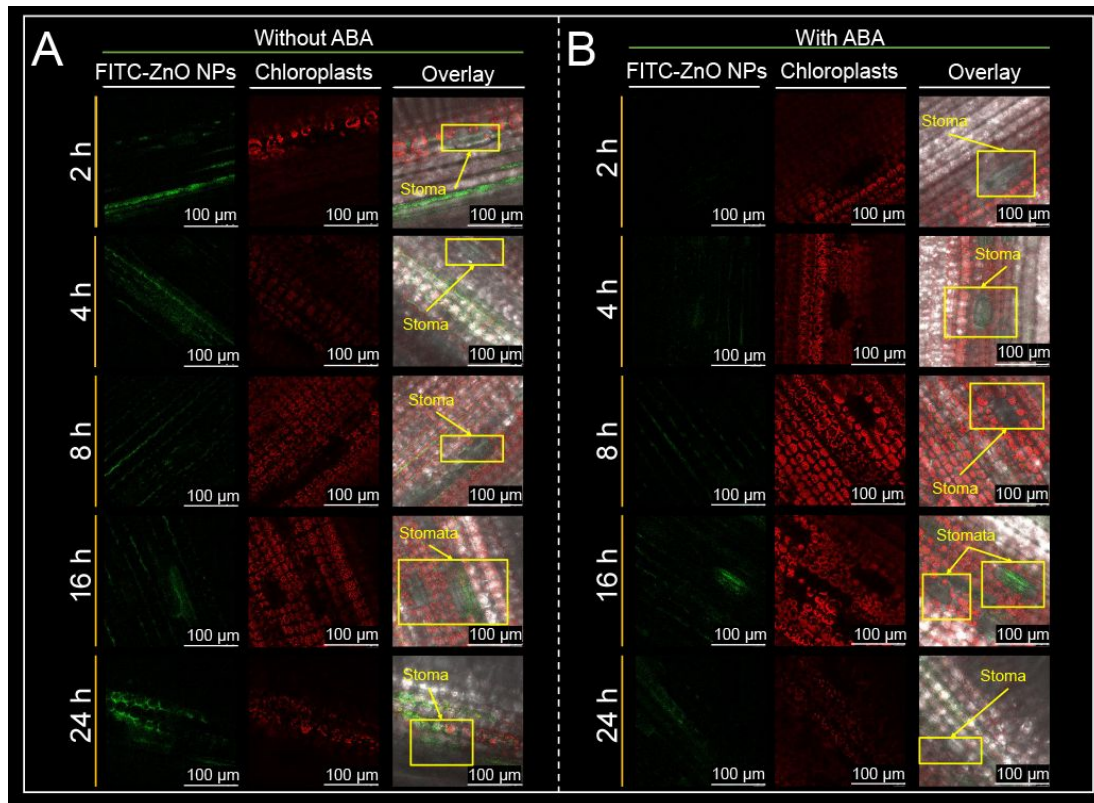


Fig. 2 Confocal laser scanning microscopy images of wheat leaves treated with (A) or without (B) $100 \mu\text{mol L}^{-1}$ abscisic acid (ABA) and sprayed with $100 \mu\text{mol L}^{-1}$ fluorescein isothiocyanate (FITC)-zinc oxide nanoparticles (FITC-ZnO NPs) at different time.

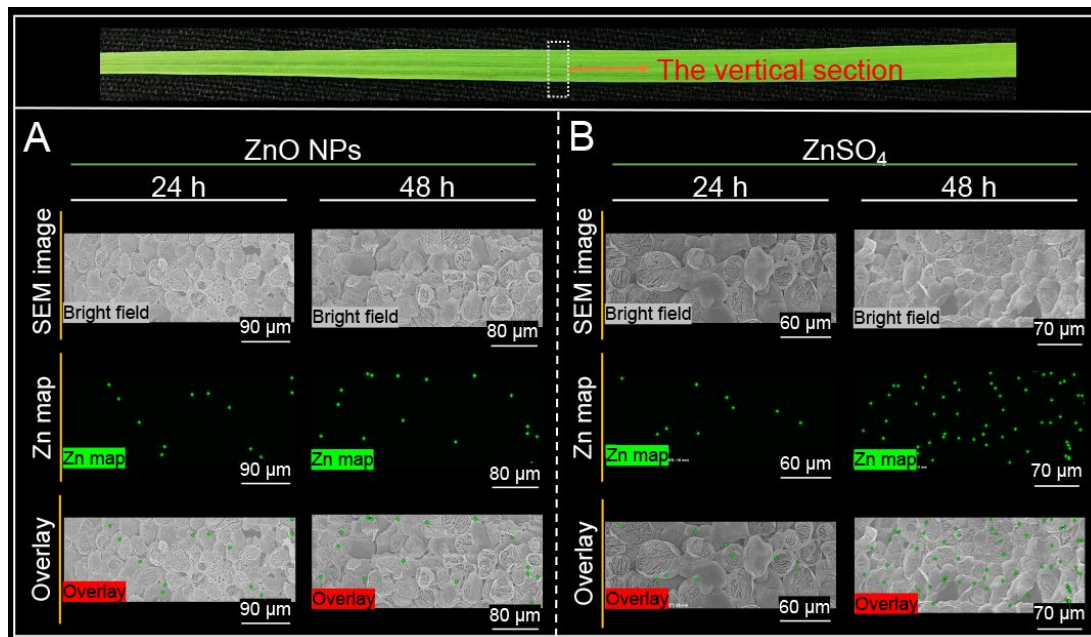
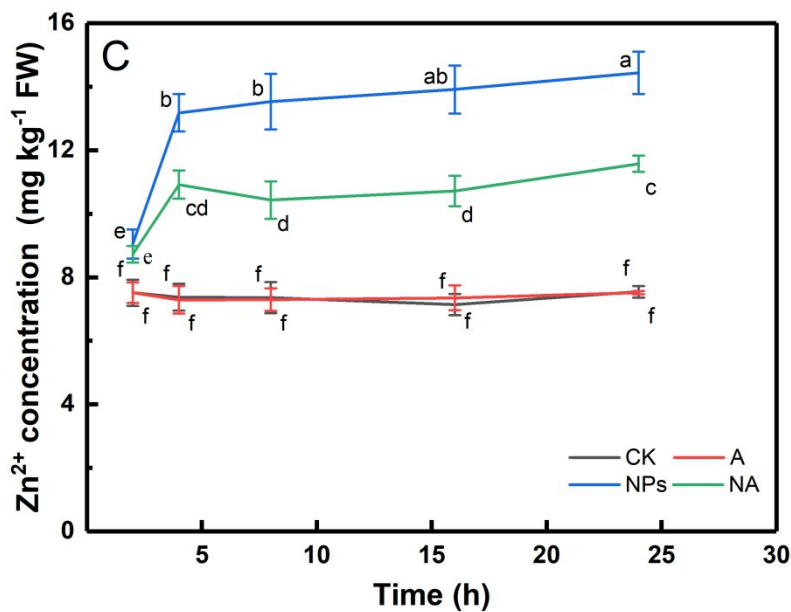
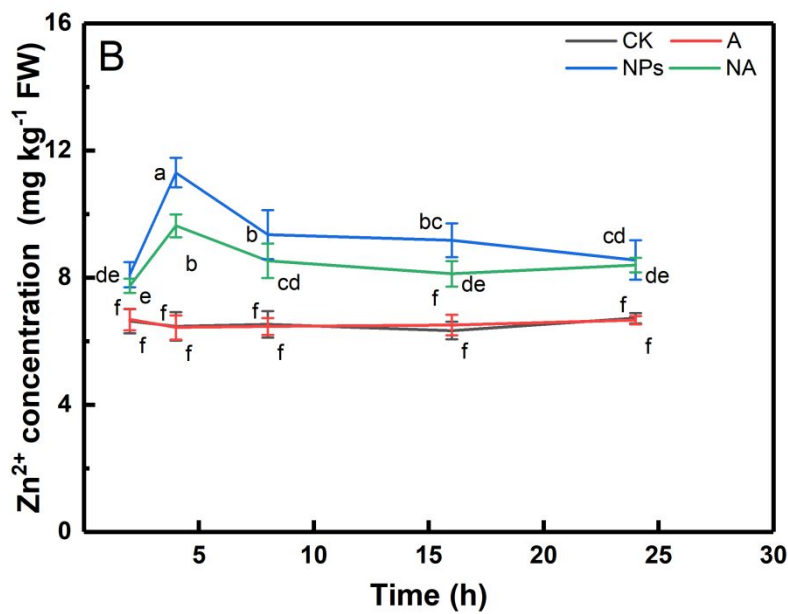
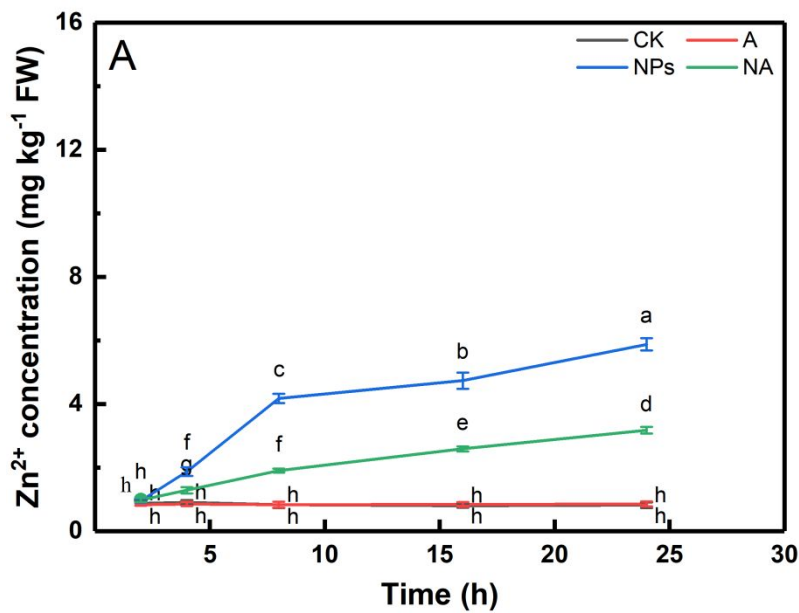


Fig. 3 Scanning electron microscope elemental mapping of wheat leaf sections treated with 1 mmol L⁻¹ zinc oxide nanoparticles (ZnO NPs) (A) and ZnSO₄ (B) for 24 and 48 h. The top of each image is close to the lower epidermis, and the bottom of each image is close to the upper epidermis.



1
2
3
4 **Fig. 4** Zn²⁺ concentrations in wheat leaf apoplast (A) cytoplasm (B) and wheat leaves (C) at
5
6 different time points. A, NPs, NA and CK present wheat leaves treated with 100 μmol L⁻¹
7
8 abscisic acid (ABA) only, 100 μmol L⁻¹ zinc oxide nanoparticles (ZnO NPs) only, 100 μmol
9
10 L⁻¹ ZnO NPs plus 100 μmol L⁻¹ ABA and deionized water, respectively. FW, fresh weight.
11
12
13
14 Data points represent mean and standard deviation values of triplicates. Different letters in
15
16 the same figure indicate significant difference at $P < 0.05$ according to *Duncan*'s test.
17
18
19
20
21
22
23
24
25
26
27
28
29
30
31
32
33
34
35
36
37
38
39
40
41
42
43
44
45
46
47
48
49
50
51
52
53
54
55
56
57
58
59
60

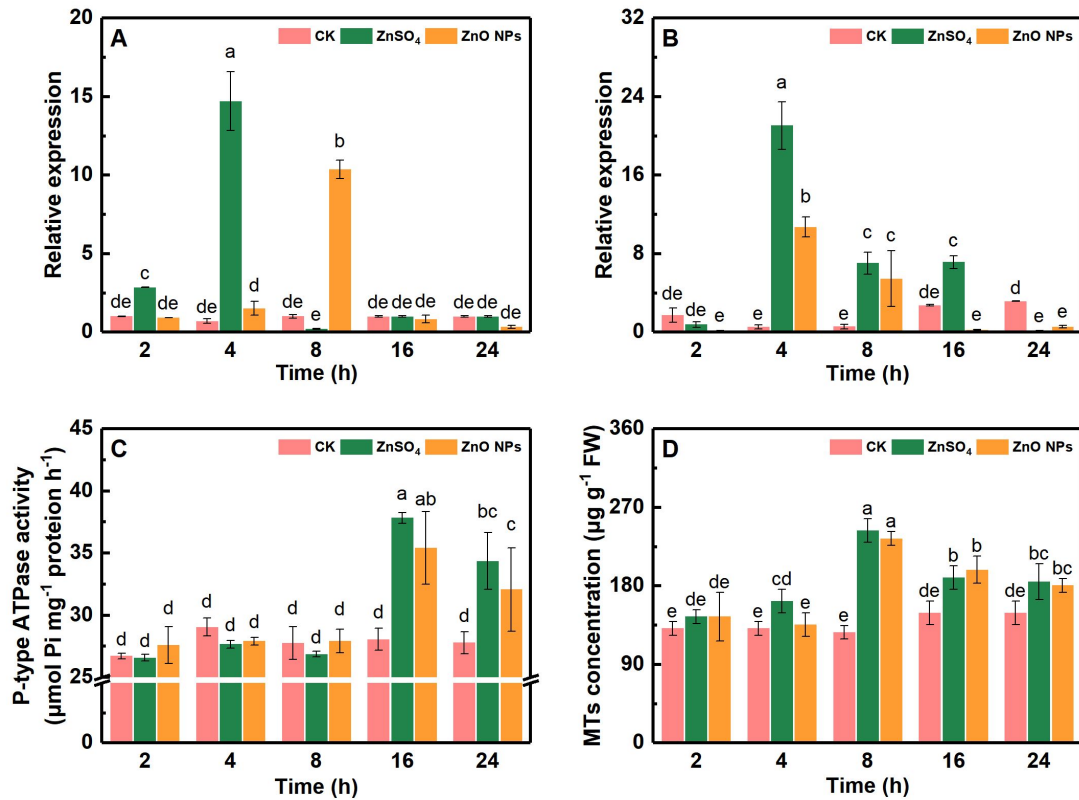


Fig. 5 Relative expression of *HAI* (A) and *Metallothionein (class II)* (B), P-type ATPase activity (C) and metallothioneins concentration (D) in different treatments (control, 100 $\mu\text{mol L}^{-1}$ ZnSO₄ solution and 100 $\mu\text{mol L}^{-1}$ zinc oxide nanoparticles (ZnO NPs) suspension) at different time in wheat leaf tissues. Pi, inorganic phosphorus. FW, fresh weight. Each histogram bar represents the mean value of triplicates. Bars are the standard deviation of the mean. Different letters on the top of columns indicate significant difference at $P < 0.05$ according to *Duncan's* test.

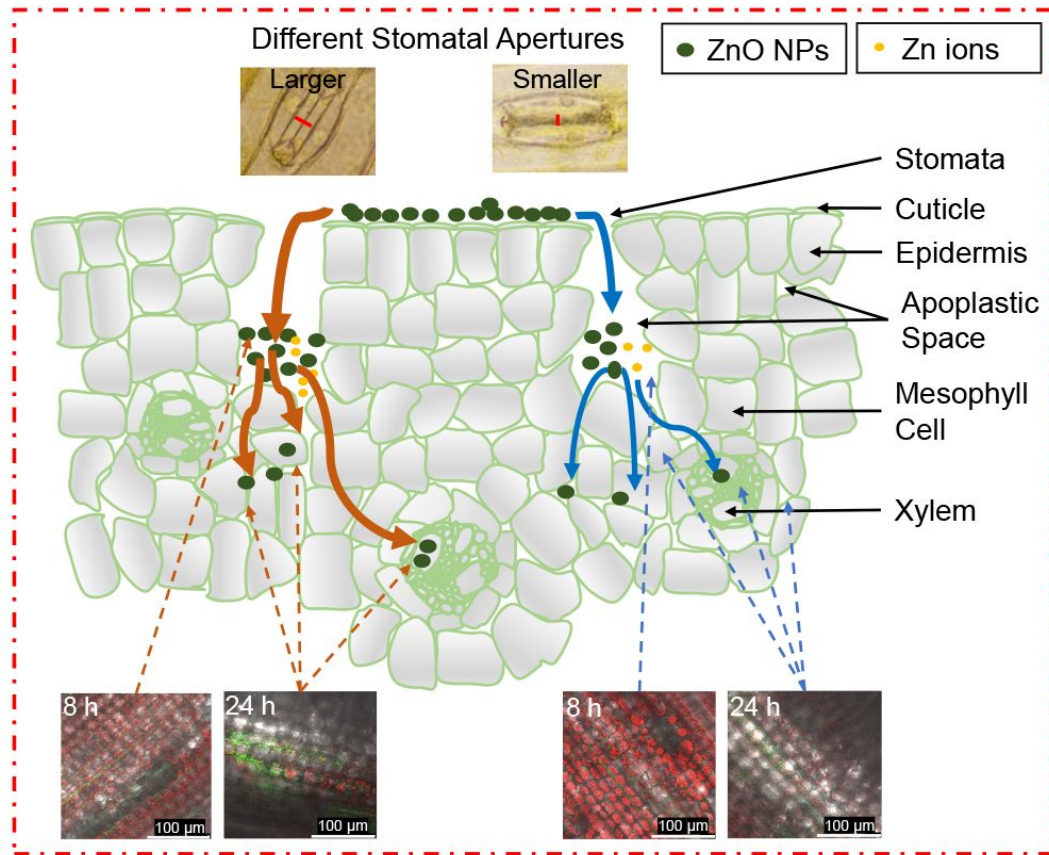
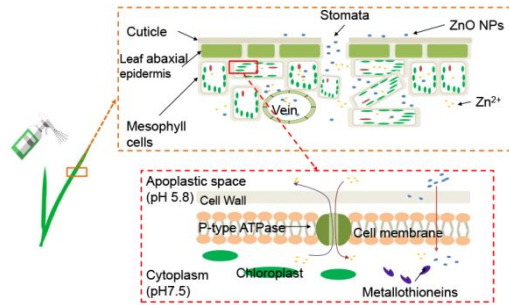


Fig. 6 ZnO NPs translocation pathways and distribution in wheat leaf with different stomatal apertures.

Table of Contents Figure



ToC text: Process of entry for ZnO NPs uptake in wheat leaves.